Thermal and Dielectric Analysis of an Ester-Based MgO Nanofluid

Manal M. Emara, *Member, IEEE*, Georgios D. Peppas, *Senior Member, IEEE*, Thomas E. Tsovilis, *Senior Member, IEEE*, Sokratis N. Tegopoulos, Apostolos Kyritsis, Eleftheria C. Pyrgioti, *Member, IEEE*, Diaa-Eldin A. Mansour, *Senior Member, IEEE*, and Ioannis F. Gonos, *Senior Member, IEEE*

***Abstract*— Magnesium oxide (MgO) nanoparticles (NPs) are used for nanofluid preparation in an effort to investigate their dielectric response and thermal properties. The matrix oil for the prepared samples is natural ester oil. Lightning impulse voltage (1.2/50 μs) is used to investigate the electrical performance of the different concentration samples. In addition, broadband dielectric spectroscopy is used for the analysis of the dielectric constant and electrical conductivity through a temperature range of 30 °C–90 °C and a frequency spectrum of 0.1 Hz–1 MHz. Thermal properties are studied by means of laser flash analysis and differential scanning calorimetry. Thermal conductivity is calculated, and the understudied results are evaluated. Results reveal an improvement in different properties for the prepared nanofluid samples, including an enhancement by 15.15% and 12.63% of the lightning impulse breakdown voltage and the thermal conductivity, respectively.**

***Index Terms*— Dielectric properties, electrical conductivity, nanofluids, nanoparticles (NPs), permittivity measurements, thermal conductivity.**

Manuscript received 24 December 2022; revised 9 April 2023 and 19 May 2023; accepted 21 August 2023. Date of publication 29 August 2023; date of current version 28 September 2023. *(Corresponding author: Manal M. Emara.)*

Manal M. Emara is with the Department of Electrical Engineering, Faculty of Engineering, Kafrelsheikh University, Kafr El-Shaikh 33511, Egypt (e-mail: manal_emara@eng.kfs.edu.eg).

Georgios D. Peppas is with Raycap S.A., 66100 Drama, Greece (e-mail: peppas@ece.upatras.gr).

Thomas E. Tsovilis is with the School of Electrical and Computer Engineering, Aristotle University of Thessaloniki, 54124 Thessaloniki, Greece (e-mail: tsovilis@auth.gr).

Sokratis N. Tegopoulos and Apostolos Kyritsis are with the School of Applied Mathematical and Physical Sciences, National Technical University of Athens, 15780 Athens, Greece (e-mail: stegopoulos@mail.ntua.gr; akyrits@central.ntua.gr).

Eleftheria C. Pyrgioti is with the Department of Electrical and Computer Engineering, University of Patras, 26504 Patras, Greece (e-mail: e.pyrgioti@ece.upatras.gr).

Diaa-Eldin A. Mansour is with the Department of Electrical Power Engineering, Faculty of Engineering, Egypt-Japan University of Science and Technology (E-JUST), Alexandria 21934, Egypt, and also with the Electrical Power and Machines Engineering Department, Faculty of Engineering, Tanta University, Tanta 31511, Egypt (e-mail: mansour@f-eng.tanta.edu.eg).

Ioannis F. Gonos is with the School of Electrical and Computer Engineering, National Technical University of Athens, 15780 Athens, Greece (e-mail: igonos@cs.ntua.gr).

Color versions of one or more figures in this article are available at https://doi.org/10.1109/TDEI.2023.3309596.

Digital Object Identifier 10.1109/TDEI.2023.3309596

I. Introduction

HIGH-VOLTAGE equipment, such as power transformers, employs numerous insulating fluids for both electrical insulation and thermal cooling purposes [1], [2]. There are many types of insulating fluids. Since the 19th century, mineral oils have been used for their merits, such as lower cost and insulating and cooling performance. Despite that, mineral oils have disadvantages, such as the harmful impact on human health due to their low biodegradability, flammability, toxicity problems, and low moisture saturation limit. In addition, they are a by-product of petroleum resources. Nowadays, it is necessary to seek alternatives to these products with natural ones.

Natural ester oils are produced from natural sources, such as plants and seeds [3]. Natural ester dielectric liquids are potentially considered as a replacement for mineral oil because of their superior performance in overcoming biodegradability and toxicity issues when using mineral oils [3], [4]. Recently, oil-based nanofluids provided another option for insulating fluids, which proved to have better thermal and dielectric properties. An effort is done in parallel by the IEEE Technical Committee on Liquid Dielectrics (TC-LD) focusing to add the nanofluids in the forthcoming IEEE and potentially IEC standards [5]. Various types, morphologies, and concentrations of nanoparticles (NPs) were used to get oil-based nanofluids with enhanced properties [6], [7], [8], [9], [10]. This enhancement is governed by the materialistic properties of NPs, including permittivity, thermal conductivity, isoelectric point, relaxation time, and so on.

Among different types of NPs, magnesium oxide (MgO) NPs were considered to be used in this study with natural ester oil due to their wide bandgap (~7.8 eV) and high electrical resistivity (10^{17} Ω·m), which enlists the MgO among the highest nanoscale oxide by means of resistivity [11], [12]. Also, MgO NPs have high thermal conductivity, good chemical and thermal stability, low cost, and excellent surface reactivity [13]. In addition, MgO NPs in nanocomposite applications have a good ability for charge trapping at their interfacing with the surrounding dielectric, thereby suppressing space charge accumulation and reflecting into improved dielectric strength [14]. The latter properties were the triggering point for considering the MgO NPs, among other oxides, into nanofluids

applications. Last but not least, the MgO NPs demonstrate low-toxicity levels [15], making them a potentially safe NPs for large-scale industrialization.

Prior art of nanofluids with MgO, focusing mainly on the ac breakdown voltage, was reported by Thomas [16], wherein a 25% ac BDV improvement was reported for the concentration of 0.005%w/w. In [17], thermally simulated current measurement was used to evaluate the quantity of trapped charges in low-density polyethylene (LDPE) and MgO/LDPE nanocomposites. It was found that MgO/LDPE nanocomposites have more trapped charges than LDPE. Consequently, the breakdown strength of these nanocomposites was increased. These results were confirmed in [18], where the mean volume density of space charge decreased after adding MgO NPs to LDPE. In [19], using MgO NPs with epoxy could increase the thermal conductivity of the nanocomposites by 75% higher than pure epoxy. In the same research, the volume resistivity and breakdown strength of MgO/epoxy nanocomposites increased by 26.8% and 11.1%, respectively, compared to pure epoxy.

For oil-based nanofluids, MgO NPs were used effectively as nanofillers with mineral oil [20]. A maximum enhancement of 69.2% was obtained at a concentration of 0.2 wt.%. MgO NPs combined with Fe_3O_4 were used in transformer oil; they proved an excellent ability to absorb and trap charges, thereby hindering the electrical discharge growth [21]. Thus, this article aims to use MgO NPs to parallelly improve the thermal along with the dielectric response of natural ester dielectric liquid. For dielectric strength, lightning impulse breakdown strength is considered instead of ac breakdown strength to cover different electrical performance parameters than already published research studies [16], [22]. Lightning impulse breakdown strength is a critical test for power transformers, as specified in IEC standard 60076-3 [23]. Following a typical approach, a needle-plane electrode configuration was used to assess lightning impulse breakdown strength [24], while dielectric constant and dielectric losses were studied.

II. Experimental Section

A. Nanofluid Preparation

Nanofluid samples were prepared using commercially obtained MgO NPs of size less than 50 nm with an ester oil of Cargill FR3. In addition to the base oil sample, only two nanofluid samples (0.006%w/w and 0.010%w/w) were prepared due to marginal change of the LIBDV and thermal conductivity, as analyzed in Section III, while further additional of NPs above 0.010%w/w would increase the risk of agglomeration [25] in the absence of surface modification. The detailed preparation procedure starts by adding the desired nanopowder amount to the corresponding oil volume. Then, oil and nanopowder were mechanically agitated for 15 min at a speed of 700 r/min. Following that, an ultrasonic homogenizer was used through two processes. The first process is the dispersion process of NPs and takes 120 min, while the second process is the degassing one and takes only 10 min to remove any produced bubbles. Ultrasonication was repeated 15–20 min prior to each experiment to ensure the proper dispersion of the nanofluids. Long-term dispersibility is a critical aspect for industrialization of nanofluids, employing various surface modification techniques (functionalization), along with dispersion stability analysis; the latter lies within the targets of our future work.

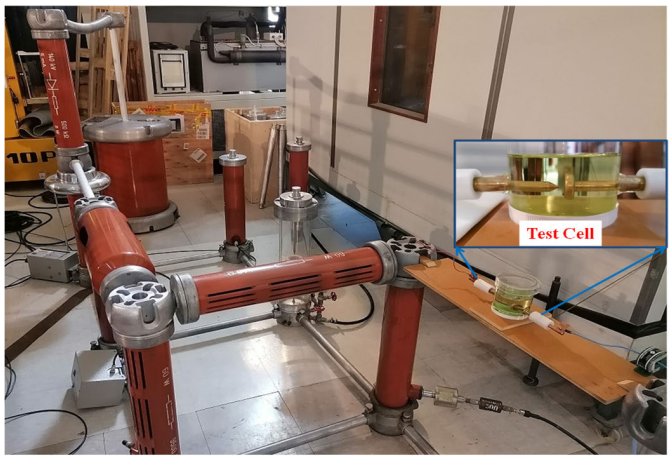

Fig. 1. Test setup and the custom-made test cell for lightning impulse voltage test setup.

B. Lightning Impulse Breakdown Voltage

Fig. 1 demonstrates the experimental setup of lightning impulse breakdown voltage measurement. The used cell consists of a needle-plane electrode with a 2.5-cm separation distance. The needle has a curvature of 50 μm radius, while the plane electrode has a diameter of 2 cm. Both electrodes are brassy. A single-stage Marx impulse voltage generator was used, providing a wave shape of 1.2-/50-μs lightning impulse voltages across the gap. A current sensor is implemented in the path to the ground to monitor the discharge current, and a capacitive divider is used to monitor the voltage. Both current and voltage are recorded digitally using a digital recorder.

Similar to previous studies [25], [26], the impulse dielectric strength was evaluated using the step-up method, in which a 2-kV step voltage was used, and three shots per step were executed. The time after each shot was set at 1 min in case of no breakdown, while it was set at 10 min in case of breakdown to exclude any residual charge affecting the test results. Once breakdown occurs, the corresponding voltage is recorded as the breakdown strength. A total of 20 shots were performed to enable statistical analysis and to obtain breakdown probability curves.

C. Thermal Properties

Heat conduction model was described in (1) [27], where the thermal conductivity (λ) was calculated considering the measured thermal diffusivity (α) along with the specific heat (c_f) as follows:

$$\lambda = \alpha c_f \rho \tag{1}$$

while ρ represents the understudied dielectric liquids matrix oil density (g/cm^3) as adopted from the suppliers' specifications of FR3 as $\rho = 0.92$ g/cm^3.

Thermal diffusivity (α) was measured by means of a NETZSCH LFA 467. The same method and techniques were

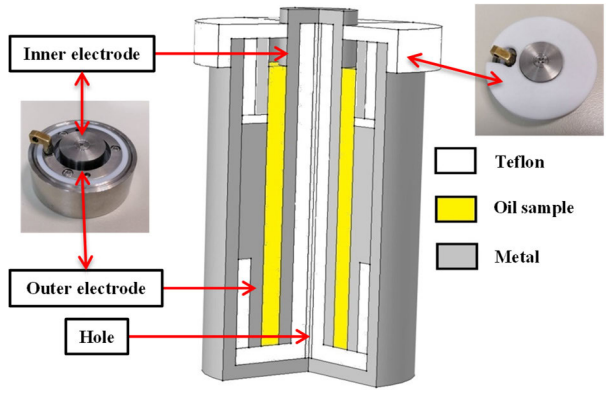

Fig. 2. DRS test cell (BDS 1307 by Novocontrol).

adopted as per [27] and [28]. Thermal diffusivity was calculated per the following equation:

$$\alpha = 1.38L^2/\pi^2 t_{1/2} \tag{2}$$

wherein L is the device under test thickness, while $t_{1/2}$ is the time to half the maximum temperature between the measuring electrodes.

Specific heat was measured using a differential scanning calorimetry (TA Instruments DSC Q200) calibrated with indium for the temperature and enthalpy and with sapphires for the heat capacity. The mass of each sample was ~10 mg and Tzero aluminum pans with hermetic lids were used to avoid any leakage. Temperature modulation was applied with a fixed temperature rise of 2 °C/min (10 °C–100 °C).

D. Dielectric Relaxation Spectroscopy

Dielectric relaxation spectroscopy was used to measure the dielectric response under a wide frequency spectrum (0.1 Hz up to 1 MHz), while heating (20 °C–100 °C) and cooling were considered to investigate the nanofluids response under various operating conditions of electrical power systems (high loads and high-/low-frequency events). The methods adopted were the same as [28] with a cylindrical test cell for dielectric liquids, as per Fig. 2.

Relative permittivity (ε_r) is calculated per

$$\varepsilon_{r(\omega)} = \varepsilon'_{r(\omega)} - j\varepsilon''_{r(\omega)} \tag{3}$$

where ε'_r is the dielectric constant and ε''_r stands for the imaginary part expressing the dielectric losses. Accordingly, electrical conductivity (σ) is calculated from

$$\sigma_{(\omega)} = \omega\varepsilon_o\varepsilon''_{r(\omega)} \tag{4}$$

where ω is the angular frequency of the wave and ε_o is the absolute dielectric permittivity of vacuum [29].

III. Results and Discussion

A. Lightning Impulse Breakdown Voltage

Fig. 3 presents a typical record of the current and voltage waveforms through breakdown conditions. It indicates that there is an initial transient current pulse at the triggering point of the Marx generator. Fig. 3 shows a sudden drop in voltage with underdamped oscillations during the breakdown conditions. In addition, a current waveform with a range of 2000 A as a secondary current is depicted following the voltage waveform pattern for breakdown occurrence.

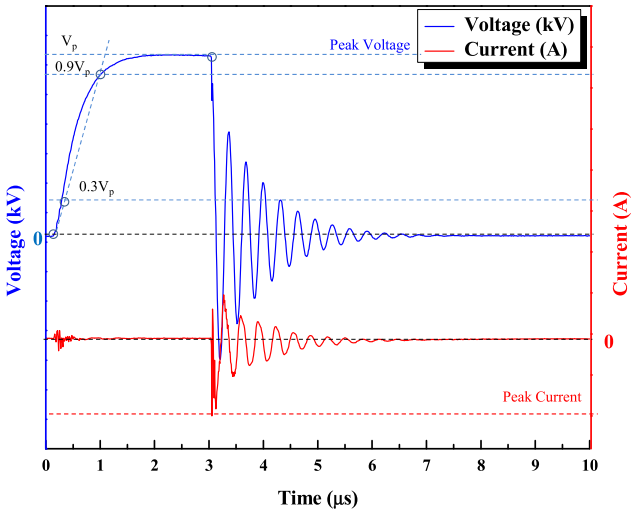

Fig. 3. Waveforms of voltage and current for breakdown conditions.

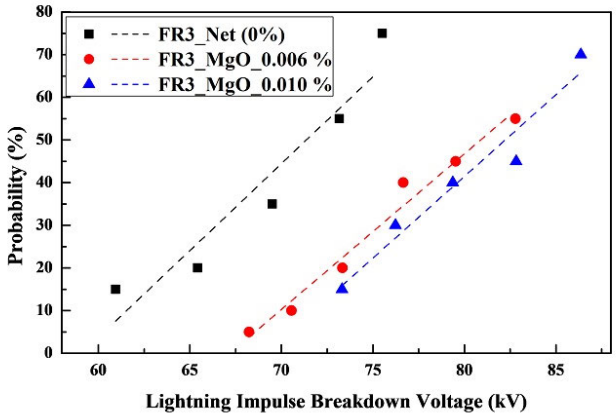

Fig. 4. Lightning impulse voltage probability of breakdown curves for the prepared samples.

Fig. 4 shows that the breakdown voltage for the probability of 50% increases based on the addition of MgO NPs from (71.43 kV, 0%w/w) to (80.89 kV, 0.006%w/w) and (82.25%w/w, 0.010%w/w). Thus, the acquired improvement was 13.24% for 0.006%w/w and 15.15% for 0.010%w/w.

B. Thermal Properties

Fig. 5 shows the thermal diffusivity results at different temperatures and concentrations. Thermal diffusivity shows a decreasing tendency by increasing the temperature, probably associated with the high effect of the interaction between the oil molecules [30]. Additionally, by increasing the nanofluid concentration, the thermal diffusivity was increased, indicating a proper dispersion of the NPs in the matrix dielectric liquid.

As mentioned in [28], the specific heat of nanofluid samples revealed similar values to the pure oil. So, specific heat was measured only for the matrix oil to be used as a base for the different samples through thermal conductivity calculations.

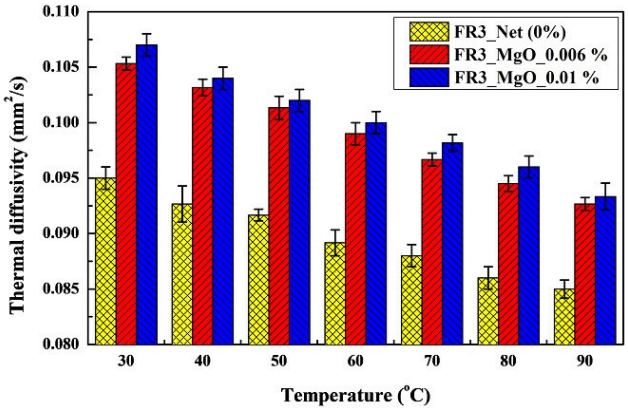

Fig. 5. Thermal diffusivity results for the prepared samples.

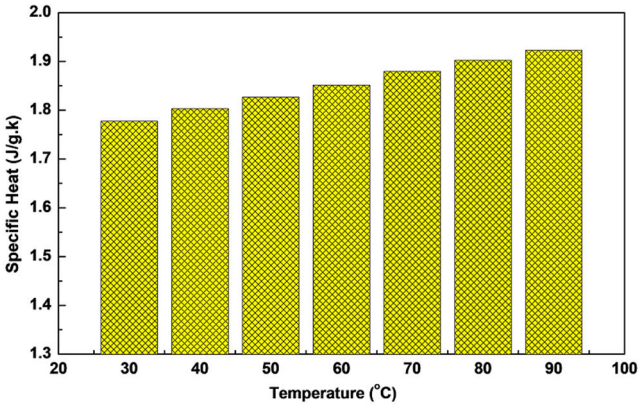

Fig. 6. Natural ester oil matrix (FR3) specific heat at different temperatures.

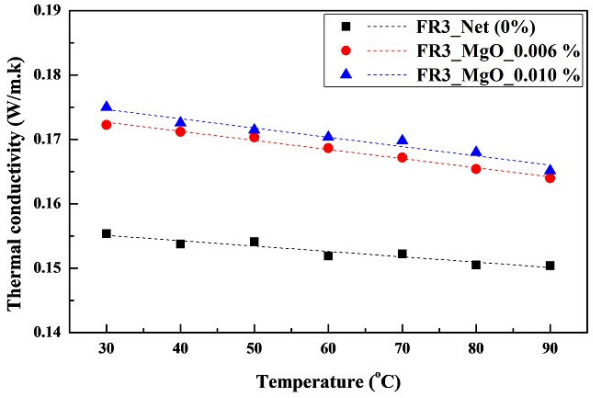

Fig. 7. Calculated thermal conductivity for different concentrations of NPs.

Fig. 6 shows the specific heat values for natural ester oil at different temperatures. It shows that the specific heat increases almost linearly against the temperature.

Fig. 7 shows the thermal conductivity results for each sample at various temperatures based on (1). It indicates that thermal conductivity increases under any increment in nanofluid concentration and decreases under any increment in temperature. The results show the enhancements for thermal conductivity that reach 10.87% for 0.006%w/w and 12.63% for 0.010%w/w at 30 °C.

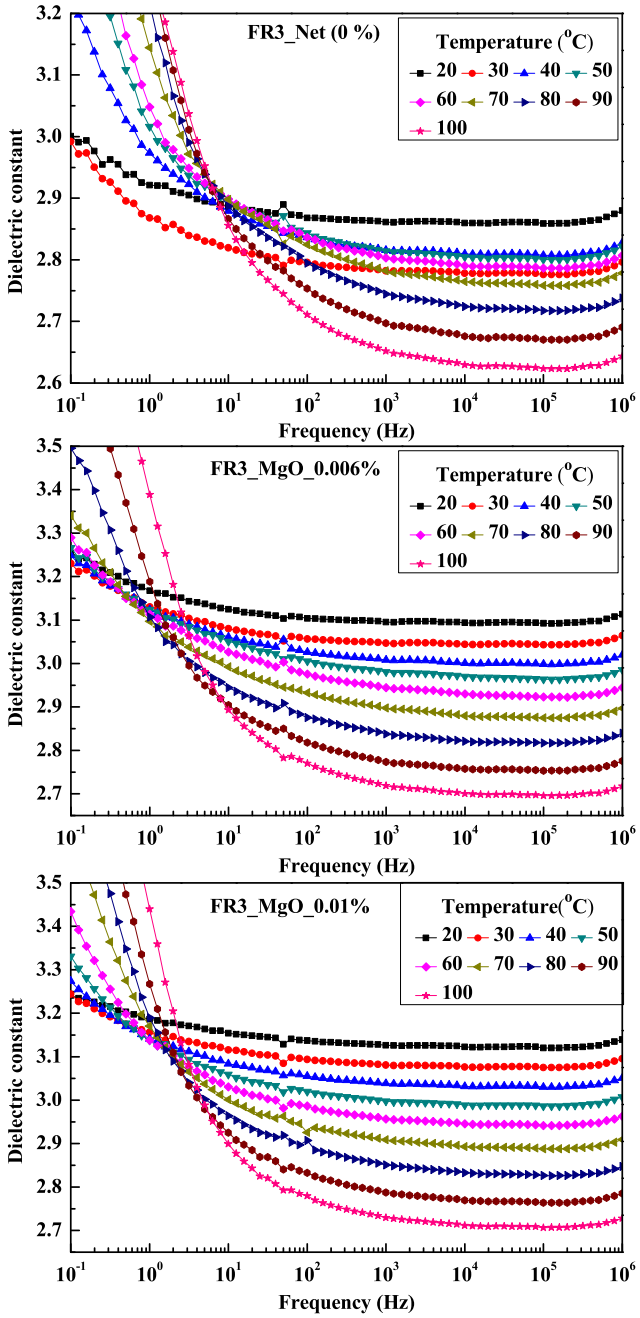

Fig. 8. Relative permittivity for the prepared samples.

C. Dielectric Relaxation Spectroscopy (Relative Dielectric Permittivity)

Fig. 8 demonstrates the understudied results of the dielectric constant in the understudied frequency spectrum, temperatures, and nanofluid concentrations. For higher frequencies (>1 kHz), relative permittivity values remain constant (frequency-independent) for all samples. In addition, it reveals enhanced values at low frequencies (~<1 kHz). The increment of the dielectric constant at the megahertz range may be an artifact in the measuring cell due to resonance effects.

As presented with the aid of Fig. 9, relative permittivity values at 1 kHz or higher frequencies decrease with any

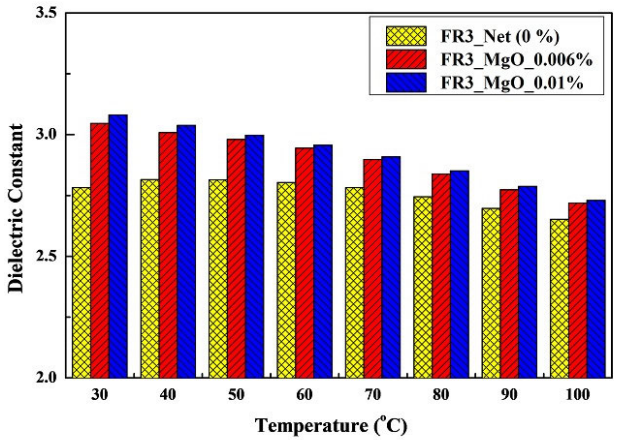

Fig. 9. Dielectric constant at different temperatures and nanofluid concentrations at 1 kHz.

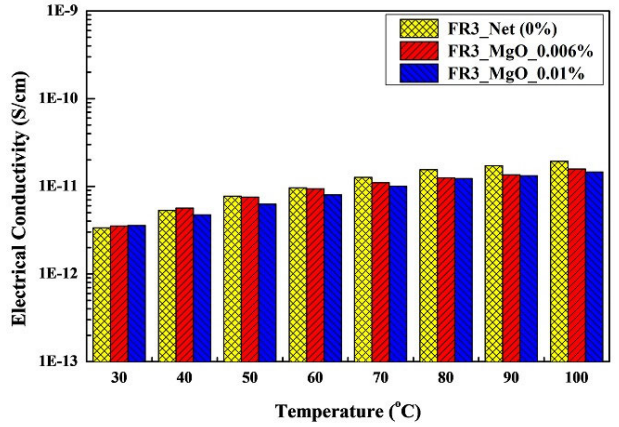

Fig. 10. Electrical conductivity at different temperatures and nanofluid concentrations at 1 kHz.

temperature increment. This effect can be described by assuming that dipolar orientation processes that scale with $1/T$ are the main contributors to the polarizability rise. In addition, enhancements in the dielectric constants are obtained under an increment in nanofluid concentration. The highest obtained enhancements at the concentration of 0.010%w/w are 9.38%, 10.66%, and 7.72% at 20 °C, 30 °C, and 40 °C, respectively.

D. Dielectric Relaxation Spectroscopy (Electrical Conductivity)

Fig. 10 indicates that electrical conductivity increases during the temperature rise for all nanofluid concentrations. Moreover, it describes that increasing nanofluid concentration leads to a decrement in electrical conductivity values. Fig. 11 reveals the studied results of electrical conductivity based on different frequencies, temperatures, and nanofluid concentrations. According to the effect of the frequency, electrical conductivity has a constant value through low-frequency region, demonstrating the activation of dc conductivity in the samples. For higher frequencies, electrical conductivity has higher values. The thermal activation process is clarified through electrical conductivity results based on increasing its values with increasing the temperature.

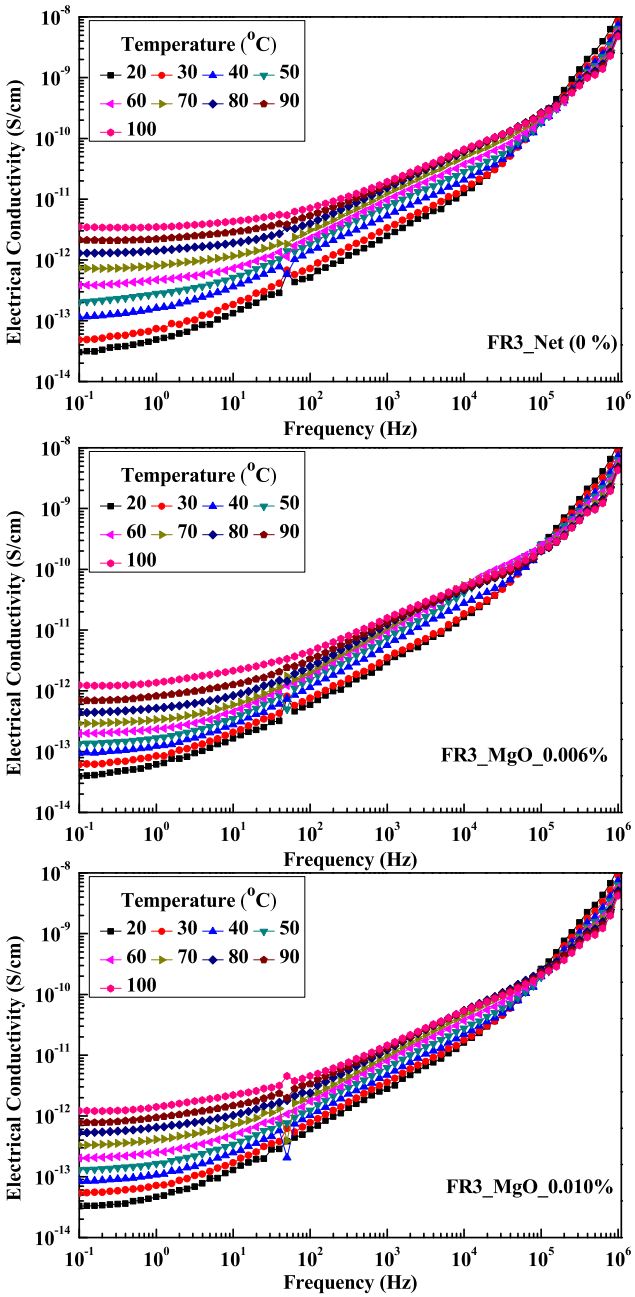

Fig. 11. Electrical conductivity for the prepared samples.

Fig. 12 represents the Arrhenius plot for dc conductivity that spectra revealed. The corresponding activation energies have been calculated for each sample. Fig. 12 shows that nanofluid samples have lower activation energies than that for the pure oil implying that the NPs modify the charge transport mechanism. This result agrees with the results obtained from lightning impulse breakdown voltage, as shown in Fig. 4. The interesting finding here is that adding the NPs reduces the dc conductivity value and, on the other hand, leads to the enhancement of the dielectric polarizability. This finding supports the interpretation that such NPs may act as traps for charge carriers, thus, improving the dielectric strength of the nanofluids.

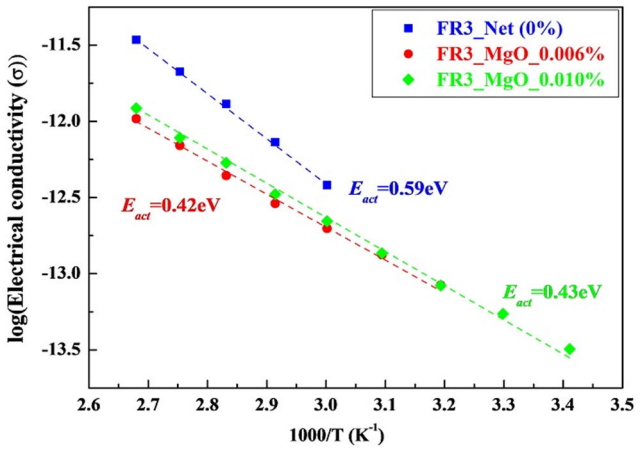

Fig. 12. Arrhenius plot for the dc conductivity recorded in the samples.

IV. Physical Discussion

In oil-based nanofluids, there are three polarization processes. The first polarization process is attributed to the polarization of oil molecules, while the second polarization process comes from the NPs themselves. The third and last polarization process is originated due to the interfacial polarization at the oil/NPs interfaces [31], [32]. From the obtained results, it is clear that nanofluids have higher dielectric constant and lower dielectric losses. This can be attributed to the confinement of some oil molecules to the surface of NPs, forming what is called an electrical double layer (EDL).

According to EDL theory, a stern layer along with a diffuse layer is formed in the vicinity of NPs when coming in contact with transformer oil [33]. With increasing temperature, the EDL thickness increases [34], causing more charges at the interfaces between NPs and oil. These charges increase ε_r' due to their role in increasing the interfacial polarization at these interfaces. At the same time, these charges became less confined to the surface, resulting in an increase in electrical conductivity. Thus, both ε_r' and electrical conductivity increase under the effect of increasing temperature. Since charges became less confined to the surface with increasing EDL thickness, they become more affected by the frequency. On the other hand, when applying high electrical fields, active electrons are generated; however, EDL acts toward hindering and trapping these electrons, thereby enhancing lightning impulse breakdown strength.

The increasing thickness of EDL against temperature (T) is positively reflected in thermal properties as follows. First, the growing thickness of EDL leads to a subsequent increase in the Brownian motion of NPs. The following formula describes how Brownian motion increases thermal conductivity [35]:

$$\frac{\lambda_{nf}}{\lambda_f} = \frac{\lambda_p + 2\lambda_f + 2\varphi(\lambda_f + \lambda_p)}{\lambda_p + 2\lambda_f - \varphi(\lambda_f + \lambda_p)} + \frac{\rho_p \varphi c_p}{2\lambda_f}\left(\sqrt{\frac{k_B T}{3\Pi r \mu_{nf}}}\right) \tag{5}$$

where λ_{nf}, λ_f, and λ_p denote the thermal conductivities of nanofluid, base fluid, and nanoparticles, respectively, φ is the volume concentration, ρ_p and c_p are the density and specific heat of nanoparticles, respectively, k_B is Boltzmann constant, r is the radius, and μ_{nf} is the nanofluid viscosity coefficient. The second term in (5) is responsible for the Brownian motion-based enhancement. Second, EDL results in a Coulomb force that repels NPs, causing them to move further and dissipate more heat. These phenomena are responsible for thermal conductivity enhancement against temperature.

V. Conclusion

In this article, MgO NPs were used to prepare natural ester (FR3)-based nanofluids with different concentrations. Lightning impulse breakdown voltage and broadband dielectric spectroscopy were used to inspect the dielectric properties of the understudied nanofluids. Thermal conductivity was used to assess the thermal response of the prepared nanofluids. The analysis revealed that using MgO NPs enhances more than 10% of the lightning dielectric strength or thermal conductivity. The results obtained from broadband dielectric spectroscopy were described and discussed in terms of the effect of different concentrations and temperatures for a wide frequency range.

Finally, proposed mechanisms were presented in an effort to describe the experimental results. The higher values for the dielectric constant and the lower values for the dielectric losses for the prepared nanofluid samples can be attributed to the formed EDL (stern and diffuse layers) around the surface of the NPs during their contact with the oil. In addition, the thickness of EDL increases by increasing the temperature resulting in forming more charges through EDL. The formed charges increase ε_r' due to the polarization effect and increase electrical conductivity due to less surface confinement. Moreover, less surface confinement made the results greatly affected by the frequency.

Acknowledgment

The authors highly acknowledge Kevin Rapp, Senior Scientist, Cargill, Brookfield, WI, USA, and Sabine Bowers from Cargill for the FR3 oil supply during this research.

References

[1] A. Beroual and H. Duzkaya, "AC and lightning impulse breakdown voltages of natural ester based fullerene nanofluids," *IEEE Trans. Dielectr. Electr. Insul.*, vol. 28, no. 6, pp. 1996–2003, Dec. 2021.

[2] S. S. M. Ghoneim et al., "Accurate insulating oil breakdown voltage model associated with different barrier effects," *Processes*, vol. 9, no. 4, p. 657, Apr. 2021.

[3] J. Jacob, P. Preetha, and T. K. Sindhu, "Stability analysis and characterization of natural ester nanofluids for transformers," *IEEE Trans. Dielectr. Electr. Insul.*, vol. 27, no. 5, pp. 1715–1723, Oct. 2020.

[4] Z. Shen, F. Wang, Z. Wang, and J. Li, "A critical review of plant-based insulating fluids for transformer: 30-year development," *Renew. Sustain. Energy Rev.*, vol. 141, May 2021, Art. no. 110783.

[5] U. M. Rao et al., "Next generation insulating liquids prepared by the international working group of IEEE DEIS technical committee on liquid dielectrics," in *Proc. IEEE 21st Int. Conf. Dielectric Liquids (ICDL)*, May 2022, pp. 1–4.

[6] A. J. Amalanathan, R. Sarathi, N. Harid, and H. Griffiths, "Investigation on flow electrification of ester-based TiO_2 nanofluids," *IEEE Trans. Dielectr. Electr. Insul.*, vol. 27, no. 5, pp. 1492–1500, Oct. 2020.

[7] G. D. P. Mahidhar, R. Sarathi, N. Taylor, and H. Edin, "Dielectric properties of silica based synthetic ester nanofluid," *IEEE Trans. Dielectr. Electr. Insul.*, vol. 27, no. 5, pp. 1508–1515, Oct. 2020.

[8] A. Beroual and U. Khaled, "Statistical investigation of lightning impulse breakdown voltage of natural and synthetic ester oils-based Fe_3O_4, Al_2O_3 and SiO_2 nanofluids," *IEEE Access*, vol. 8, pp. 112615–112623, 2020.

[9] H. Khelifa, E. Vagnon, and A. Beroual, "AC breakdown voltage and partial discharge activity in synthetic ester-based fullerene and graphene nanofluids," *IEEE Access*, vol. 10, pp. 5620–5634, 2022.

[10] H. Cong, H. Shao, Y. Du, X. Hu, W. Zhao, and Q. Li, "Influence of nanoparticles on long-term thermal stability of vegetable insulating oil," *IEEE Trans. Dielectr. Electr. Insul.*, vol. 29, no. 5, pp. 1642–1650, Oct. 2022.

[11] T. Maezawa et al., "Space charge formation in LDPE/MgO nanocomposite under high electric field at high temperature," in *Proc. Annu. Rep.-Conf. Electr. Insul. Dielectric Phenomena*, 2007, pp. 271–274.

[12] S. A. Canney, V. A. Sashin, M. J. Ford, and A. S. Kheifets, "Electronic band structure of magnesium and magnesium oxide: Experiment and theory," *J. Phys., Condens. Matter*, vol. 11, no. 39, pp. 7507–7522, Oct. 1999.

[13] S. Abinaya, H. P. Kavitha, M. Prakash, and A. Muthukrishnaraj, "Green synthesis of magnesium oxide nanoparticles and its applications: A review," *Sustain. Chem. Pharmacy*, vol. 19, Apr. 2021, Art. no. 100368.

[14] T. Andritsch, R. Kochetov, P. H. F. Morshuis, and J. J. Smit, "Dielectric properties and space charge behavior of MgO-epoxy nanocomposites," in *Proc. 10th IEEE Int. Conf. Solid Dielectrics*, Jul. 2010, pp. 1–4.

[15] S. Ge et al., "Cytotoxic effects of MgO nanoparticles on human umbilical vein endothelial cells in vitro," *IET Nanobiotechnol.*, vol. 5, no. 2, pp. 36–40, Jun. 2011.

[16] P. Thomas, "Breakdown voltage and gassing tendency of synthetic esters based MgO nanofluids," in *Proc. IEEE 4th Int. Conf. Condition Assessment Techn. Electr. Syst. (CATCON)*, Nov. 2019, pp. 1–3.

[17] S. Peng, J. He, J. Hu, X. Huang, and P. Jiang, "Influence of functionalized MgO nanoparticles on electrical properties of polyethylene nanocomposites," *IEEE Trans. Dielectr. Electr. Insul.*, vol. 22, no. 3, pp. 1512–1519, Jun. 2015.

[18] V. Wang, J. Wu, and Y. Yin, "Nanostructures and space charge characteristics of MgO/LDPE nanocomposites," *IEEE Trans. Dielectr. Electr. Insul.*, vol. 24, no. 4, pp. 2390–2399, 2017.

[19] G. Ge, Y. Tang, Y. Li, and L. Huang, "Effect of environmental temperature on the insulating performance of Epoxy/MgO nanocomposites," *Appl. Sci.*, vol. 10, no. 20, p. 7018, Oct. 2020.

[20] A. Katiyar, P. Dhar, T. Nandi, and S. K. Das, "Effects of nanostructure permittivity and dimensions on the increased dielectric strength of nano insulating oils," *Colloids Surf. A, Physicochemical Eng. Aspects*, vol. 509, pp. 235–243, Nov. 2016.

[21] A. Thabet, M. Allam, and S. A. Shaaban, "Investigation on enhancing breakdown voltages of transformer oil nanofluids using multi-nanoparticles technique," *IET Gener., Transmiss. Distrib.*, vol. 12, no. 5, pp. 1171–1176, Mar. 2018.

[22] A. B. Afzal, Z. A. Noorden, and A. B. Afzal, "A simulation study on electrical and thermal properties of nanofluids based mineral oils for potential transformer applications," *IEEE Trans. Dielectr. Electr. Insul.*, vol. 29, no. 6, pp. 2312–2319, Dec. 2022.

[23] *Part 3. Insulation Levels, Dielectric Tests and External Clearances in Air*, Standard IEC 60076-3, 2000.

[24] Y. V. Thien, N. Azis, J. Jasni, R. Yunus, M. Z. A. A. Kadir, and Z. Yaakub, "Influence of electrode geometry on the lightning impulse breakdown voltage of palm oil," in *Proc. IEEE PES Asia–Pacific Power Energy Eng. Conf. (APPEEC)*, Oct. 2018, pp. 317–320.

[25] M. M. Emara, G. D. Peppas, T. E. Tsovilis, E. C. Pyrgioti, and I. F. Gonos, "Lightning impulse performance of natural ester oil based nanofluid with magnesium oxide nanoparticles," in *Proc. 22nd Int. Symp. High Voltage Eng. (ISH)*, vol. 2021, Nov. 2021, pp. 1593–1596.

[26] M. M. Emara et al., "Dielectric and thermal performance of natural ester oil based nanofluid with magnesium oxide nanoparticles," in *Proc. IEEE 21st Int. Conf. Dielectric Liquids (ICDL)*, May 2022, pp. 1–6.

[27] P. A. Klonos, S. N. Tegopoulos, C. S. Koutsiara, E. Kontou, P. Pissis, and A. Kyritsis, "Effects of CNTs on thermal transitions, thermal diffusivity and electrical conductivity in nanocomposites: Comparison between an amorphous and a semicrystalline polymer matrix," *Soft Matter*, vol. 15, no. 8, pp. 1813–1824, 2019.

[28] M. M. Emara et al., "Thermal and dielectric performance of ester oil-based pentyl-graphene nanofluids," *IEEE Trans. Dielectr. Electr. Insul.*, vol. 29, no. 2, pp. 510–518, Apr. 2022.

[29] M. M. Emara, D. A. Mansour, and A. M. Azmy, "Mitigating the impact of aging byproducts in transformer oil using TiO_2 nanofillers," *IEEE Trans. Dielectr. Electr. Insul.*, vol. 24, no. 6, pp. 3471–3480, Dec. 2017.

[30] H. J. Wang, S. J. Ma, H. M. Yu, Q. Zhang, C. M. Guo, and P. Wang, "Thermal conductivity of transformer oil from 253 K to 363 K," *Petroleum Sci. Technol.*, vol. 32, no. 17, pp. 2143–2150, Sep. 2014.

[31] J. Miao, M. Dong, M. Ren, X. Wu, L. Shen, and H. Wang, "Effect of nanoparticle polarization on relative permittivity of transformer oil-based nanofluids," *J. Appl. Phys.*, vol. 113, no. 20, May 2013.

[32] R. A. Farade et al., "The effect of interfacial zone due to nanoparticle-surfactant interaction on dielectric properties of vegetable oil based nanofluids," *IEEE Access*, vol. 9, pp. 107033–107045, 2021.

[33] N. Ise and I. Sogami, *Structure Formation in Solution: Ionic Polymers and Colloidal Particles*. Berlin, Germany: Springer, 2005.

[34] H. Saboorian-Jooybari and Z. Chen, "Calculation of re-defined electrical double layer thickness in symmetrical electrolyte solutions," *Results Phys.*, vol. 15, Dec. 2019, Art. no. 102501.

[35] J.-M. Liu, Z.-H. Liu, and Y.-J. Chen, "Experiment and calculation of the thermal conductivity of nanofluid under electric field," *Int. J. Heat Mass Transf.*, vol. 107, pp. 6–12, Apr. 2017.

Manal M. Emara (Member, IEEE) was born in Kafr El-Shaikh, Egypt, in 1989. She received the B.Sc. and M.Sc. degrees in electrical power and machines engineering from Kafrelsheikh University, Kafr El-Shaikh, and Tanta University, Tanta, Egypt, in 2011 and 2016, respectively, and the Ph.D. degree from the School of Electrical Computer Engineering, National Technical University of Athens (NTUA), Athens, Greece, in 2021.

She has been with the Electrical Engineering Department, Kafrelsheikh University, since 2012, where she is currently an Assistant Professor. Her research interests include high-voltage engineering and nanodielectric materials.

Georgios D. Peppas (Senior Member, IEEE) was born in Rustenburg, South Africa, in 1987. He received the Diploma degree in electrical engineering and the Ph.D. degree from the Department of Electrical and Computer Engineering, University of Patras, Patras, Greece, in 2011 and 2016, respectively.

He is currently the Research and Development Manager of Raycap S.A., Drama, Greece, leading innovation in surge protective devices, and the Technical Manager of the High Current Laboratory, Raycap S.A. He is the author of more than 45 papers in major scientific journals and conference proceedings. He holds seven patents. His research interests include lightning and surge protection and nanofluids for high-voltage applications.

Thomas E. Tsovilis (Senior Member, IEEE) was born in Piraeus, Greece, in 1983. He received the M.Eng. and Ph.D. degrees in electrical and computer engineering from the Aristotle University of Thessaloniki (AUTh), Thessaloniki, Greece, in 2005 and 2010, respectively.

He was the Director of High Current Laboratories, Raycap S.A., Drama, Greece, and Komenda, Slovenia, from 2012 to 2018. In 2018, he joined AUTh, where he is currently an Assistant Professor. He is the author of more than 80 publications in leading scientific journals and international conferences. He is the inventor of eight granted U.S. patents on surge protective devices and testing techniques. His research interests include the broad area of high-voltage engineering with emphasis given to electrical discharges, lightning protection, and insulation coordination for power systems.

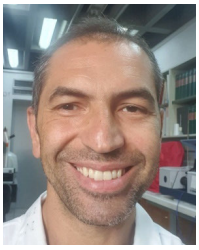

Sokratis N. Tegopoulos was born in Athens, Greece, in 1977. He received the B.Sc. degree in natural sciences from Hellenic Open University, Patras, Greece, in 2016, and the M.Sc. degree in applied physics from the School of Applied Mathematical and Physical Sciences, National Technical University of Athens (NTUA), Athens, in 2018, where he is currently pursuing the Ph.D. degree.

Within the research activity of the Dielectrics Group, he participates in research projects and assists in teaching undergraduate and postgraduate students. His research interests include the study of structure–properties relationship in (bio)polymer nanocomposite materials.

Apostolos Kyritsis was born in Berlin, Germany, in 1966. He received the Diploma degree in physics and the Ph.D. degree in materials science-physics from the University of Athens, Athens, Greece, in 1988 and 1995, respectively.

He is currently an Associate Professor with the National Technical University of Athens (NTUA), Athens. He has published more than 150 scientific articles in major international peer-reviewed scientific journals and five book chapters. He has more than 200 contributions to international conferences and more than 50 contributions to national conferences. His scientific interests include dielectric, thermal, and vapor sorption studies in ionic crystals, ceramics, polymers and complex polymeric systems, and structure–property relationships in polymers, biopolymers, nanocomposites, and hydration properties of inorganic and organic materials.

Eleftheria C. Pyrgioti (Member, IEEE) was born in Kanalia, Karditsa, Greece, in 1958. She received the Diploma degree in electrical engineering and the Ph.D. degree from the Electrical and Computer Engineering Department, University of Patras, Patras, Greece, in 1981 and 1991, respectively.

She is currently a Professor with the Electrical and Computer Engineering Department, University of Patras. Her research interests include high-voltage systems, lightning protection, high-voltage insulation, dielectric liquids distributed generation, and renewable energy.

Diaa-Eldin A. Mansour (Senior Member, IEEE) was born in Tanta, Egypt in 1978. He received the B.Sc. and M.Sc. degrees in electrical engineering from Tanta University, Tanta, Egypt, in 2000 and 2004, respectively, and the Ph.D. degree in electrical engineering from Nagoya University, Nagoya, Japan, in 2010.

Since 2000, he has been with the Department of Electrical Power and Machines Engineering, Faculty of Engineering, Tanta University, Egypt, where he has been a professor since 2020. He is currently working as a professor in Electrical Power Engineering Department, Egypt-Japan University of Science and Technology (E-JUST), Alexandria, Egypt, on leave from Tanta University. His research interests include high voltage engineering, condition monitoring of electrical power equipment, IoT applications in electrical power systems, and applied superconductivity.

Dr. Mansour received the Best Presentation Award two times from IEE of Japan in 2008 and 2009, Prof. Khalifa's Prize from the Egyptian Academy of Scientific Research and Technology in 2013, the Tanta University Encouragement Award in 2016, and the Egypt-State Encouragement Award in the field of engineering sciences in 2018. Recently, he has been listed among the world's top 2% scientists by Stanford University, USA, in 2020, 2021 and 2022.

Ioannis F. Gonos (Senior Member, IEEE) was born in Artemisio, Arcadia, Greece, in 1970. He received the Diploma degree in electrical engineering and the Ph.D. degree from the National Technical University of Athens (NTUA), Athens, Greece, in 1993 and 2002, respectively.

He is currently a Professor with NTUA. He is the author of more than 200 papers in scientific journals and conferences proceedings. His research interests include grounding systems, dielectric liquids, high voltages, measurements, and insulators.